Applied Mathematics & Information Sciences
An International Journal

http://dx.doi.org/10.18576/amis/150315

Vibration Analysis of Permanent Magnet Motor Rotor System in Shearer Semi-Direct Drive Cutting Unite with Speed Controller and Multi- Excitation Forces

Y. A. Amer[1], *Taher A. Bahnasy*[2,*] *and Ashraf M. Elmhlawy*[2]

[1]Department of Mathematics, Faculty of Science, Zagazig University, Zagazig, Egypt
[2]Department of Physics and Engineering Mathematics, Faculty of Engineering, Tanta University, Tanta, Egypt

Received: 11 Mar. 2021, Revised: 5 Apr. 2021, Accepted: 11 Apr. 2021
Published online: 1 May 2021

Abstract: Under the impact of electro - magnetic activation and marginal load disruption, electro - mechanical linking resonance can be generated on the motor driveshaft of the moderately slicing segment of a shearer. In this sense, this hypothesis explores the vibration properties of a motor rotor and the effect of electro - mechanical couplers. Besides, system model approximate solution is obtained through the multiple time scales method in the instance of sub-harmonic resonance, and the Rung-Kutta Procedure of the fourth order defined the steady-state solution. In addition, the electric and magnetic factors containing the angle of the operational strength factor, the couple of pole combinations, the permanent magnet index, the saturation magnetization correlation and the technical parameters concerned for the tensile vibrations of the rotor structure, such as torsional rotor stiffness and longitudinal load, are tested. In considering Lyapunov's first indirect procedure, the equilibrium of the steady state approach nearby its worst resonance situation is reviewed. The results on the steady state solution of the various parameters are surveyed and discussed. The simulation outcomes are calculated using the software MATLAB program.

Keywords: Electromagnetic excitation disturbance, Electromechanical coupling resonance, Shearer semi-direct cutting section, Multiple time scales method, Sub-harmonic resonance, Active feedback controller, Stability analysis

1 Introduction

A three-phase induction motor, a radial transmitting system, a thrust gear driving system, and radial drums are indications of the traditional cutting structure of a shearer[1,2]. Limited speed control performance, the long transmission joint in the breaking portion, and a rising failure rate are the drawbacks. A permanent semi-direct magnetic shearer transmitting mechanism in which the planetary gear is eliminated and a permanent magnet synchronous motor (PMSM) is included instead of the induction motor as the driving root motor is implemented in this study. A middle spur gear transmission device is responsible for the transfer of the driving torque generated by this process to the terminal drum. As the terminals drum separates the coal walls [3,4,5], the stresses and dynamic loading can be confronted by this gear shift process. Thus, the electro - magnetic shearer rotor performance efficiency and terminal load specifications may have a far-reaching impact on the reliability and functionality of the shearer transmission device. The semi-direct transmission mechanism of the coal cutting tool usually corresponds to the electro - mechanical linking system [6,7,8], where there can be abundant dynamic properties [9,10,11].

Different terminal loads will relay several variations in the interactive output of the driving motor, causing intensification to the chaotic behavior of the structure. The machinery drops its balance mainly when the operating motor's revolving speed is equivalent to or exceeds the critical rotation speed of the transmitting system's dynamic modules and the resonance phenomena is likely to occur [12,13]. Therefore, by taking complete consideration of the consequence of linking between machinery; electric and magnets impacts, it is essential to clarify the vibration in the transmitted rotor shaft

* Corresponding author e-mail: taher.bahnasy@gmail.com; Taher.Bahnasy@f-eng.tanta.edu.eg

structure. It is also recommended to investigate the vibration dynamic behavior with the essence of mechanical and electromagnetic linking in such an operating and boundary state to realise the electro - magnetic synchronization mechanism. To present, more trials have been carried out on the respective research between electronic and mechanical structures in relation to the complex features of electro - mechanical connection than on the examination of the coal screw operating brake system apparatus, which impedes the development of certain problems in the joint zones of the mechanism. Considering that, it was possible to effectively experience the mixing behavior of electro-mechanics on massive spinning devices.

As one of the pioneers in describing the electric and magnetic behavior of the induction machine as well as the oscillatory and radial noise of the gears, Yi et al. [14] investigated the dynamic model of the multi-stage planetary gear set with electric drive, from which the electro - mechanical interface scheme was researched. The servo drive and mechanical structure analytical model for electromechanical connection was developed by Yang et al. [15]. The impacts of churn modulations was concluded and the response features of thrust harmonics and rotary materials were calculated for the precision of functional configuration. Xu and Gao [16] have continued their research of the nonlinear interacting magnetic energy of the driving motor in an electromagnetic module. Furthermore the nonlinear mechanical and electrical interaction formula was indicated for the moveable system, whereby bifurcation and aggressive conduct were also verified. According to Bai et al.[17], a complex process for the electromagnetic procedure, which combines the nonlinear permeability network design of such a squirrel-cage induction machine and the connecting lateral torsional impact of a terrestrial geared rotor device, has been clarified. In addition, the outcomes of the dynamic features were considered.

A dynamic mechanical and electrical synchronization model for revolving machines was developed by Szolc et al. [18]. He investigated the influence of electrodynamic flexural and damping correction factor on the machine tool. The above-mentioned studies, show that the torsional vibration patterns of the electromagnetic conductivity device and its linking function have been both severely and concisely reviewed. Only a few investigations on electromechanical disruption have been performed, while the system is under electromagnetic perturbation and parameter disturbance. Electro - mechanical resonance mediated process instability may have far-reaching impacts on the stable operation of the semi-direct driving system. For this interface, in production electrical equipment, Calleecharan and Aidanpää[19], Gustavsson and Aidanpää[20], Lundström and Aidanpää[21] have made considerable struggles to obtain an erratic magnetic pulling driven by eccentricity. The kernel of electromagnetism rigidity was developed by Song and Ma [22] with considerable determination on the magnetic potential model in the air gaps of a hydro-generator reactor, where its influences on the critical speed of the rotor were indicated on the basis of the Lyapunov stability concept. Hang et al. [23] explicitly discussed the intermittent, quasi-periodic as well as erratic movements of the irregular rotor parameter variation of the generator. Ran et al. [24] examined electromechanical recombination through a twofold induction system fitted with a screw. The results showed that the shaft vibration could be prevented by the decrease in negative dissipation by the electrostatic controller. The exploratory experiments performed by Zhong and Tang [25] found that throughout the high-speed rolling process, certain forms of disturbances can have certain relationships mostly with adaptive recombination.

A complex behaviour formulation of the spinning configuration was constructed to explore the features of negative performance modulation and vertical personality vibrations. In view of the inconsistency of rotating structures of spinning machinery, Gan et al. [26] extended the non-parametric modelling technique to the unspecified Jeffcott rotor with disk split and the demonstrated randomized simulation model. In order to target the torsional disturbance in the electromechanical transmission device, the active vibration method was advanced and the disturbance characteristics were reviewed by Chen et al. [27] on the condition of exterior excitation. Although there is a significant number of publications in electromechanical synchronization structures on resonance problem, it focuses more on the situation of eccentricity in the configuration of the drive shaft. The actual load of the mechanism and the load linking and electromagnetic activation are not considered. The nonlinear disturbance control is explored employing a specific nonlinear modified positive position feedback (MPPF) approach by Y.S. Hamed et al. [28] for a cantilever beam structure carrying an underlying lumped mass.

In this article, the non - linear dynamic algorithm of the rotor system is analyzed with multi-excitation forces, and with electromagnetic interference and terminal load interruption is considered. To reduce the induced vibrations on the resonance cases, the impact of negative velocity and cubic velocity feedback controller is created. In addition, in the instance of sub-harmonic resonance, in order to find the approximate solution of this model, a multiple time scales scheme is included and its stability is often determined by a computational procedure. Moreover, electromagnetic parameters are being tested. Some feedback on the different module specifications is documented and the controller's consequences on the system's performance are numerically reported. Comparisons are reported with the numerical solution.

2 Mathematical analysis and system model

A PMSM, a three-stage spur mechanism reducer, including a variable-frequency radial cutting drum ride controller comprising of the semi-direct shearer drive cutting transmitting module demonstrated in Figure 1 [29]. The electromechanical connectivity transmitting scheme of the shearer is formulated into a two-inertia torsional vibration mechanism which comprises a PMSM and a cutting drum via a linking shaft, as indicated in Figure 2. In this paper, by introducing multi-excitation forces, we established the mathematical model given in [29] and discussed the effect of negative velocity and cubic velocity feedback controller on the resonance cases on the reduction of induced vibrations. According to these considerations, the mathematical model for the system will be

$$\ddot{x}+\omega^2 x=-\varepsilon\mu\dot{x}-\varepsilon\gamma x^2-\varepsilon\alpha x^3+f_1\varepsilon\cos(\Omega_1 t)+ f_2\varepsilon x\cos(\Omega_2 t)-\varepsilon k_1\dot{x} \tag{1}$$

where

$$\omega=\sqrt{1-\frac{k_1 J_2}{J_1(J_1+J_2)\omega_o^2}},\ \mu=\frac{C(J_1+J_2)}{J_1 J_2\omega_o^2},\ \gamma=\frac{k_2}{J_1\omega_o^2}\left(\frac{J_2}{J_1+J_2}\right)^2,\ \alpha=\frac{k_3}{J_1\omega_o^2}\left(\frac{J_2}{J_1+J_2}\right)^3,\ \omega_o=\sqrt{\frac{K(J_1+J_2)}{J_1 J_2}}, \tag{2}$$

, k_n , $n=1,2,3$ are parameters dependent on essential magnitude of the permanent magnet, the permeability of the PMSM air gap, number of motor poles, and magnetic field intensity of the stator, J_1 , J_2 are the PMSM and the corresponding cutting drum moment of inertia, respectively, ω_o , Ω_i , $i=1,2$ are the internal and external excitation frequencies respectively, $C$is the mechanical damping of the flexible shafting, $K$is the linear torsional rigidity of the elastic shafting mechanism.

Applying the method of multiple time scales (MTSM), of $U(t)$ and $V(t)$ in power series form as:

$$x(T_o, T_1, ..., T_n, \varepsilon)=\sum_{n=0}^{\infty}\varepsilon^n x_n \tag{3}$$

where the time derivative takes the values:

$$\frac{d}{dt}=D_0+\varepsilon D_1+O(\varepsilon^2),\ \frac{d^2}{dt^2}=D_o^2+2\varepsilon D_0 D_1+O(\varepsilon^2) \tag{4}$$

and $T_n=\varepsilon^n t$, $D_n=\frac{\partial}{\partial T_n}$.

Applying equations (3), (4) into (**??**) and equating same power of ε coefficients to have:

$$O(\varepsilon^0): \quad (D_o^2+\omega^2)x_0=0, \tag{5}$$

$$O(\varepsilon): \quad (D_o^2+\omega^2)x_1=-2D_o D_1 x_o-\mu D_o x_o-\gamma x_0^2-\alpha x_0^3+f_1\cos(\Omega_1 t)+f_2 x_o\cos(\Omega_2 t)-k_1 D_o x_o \tag{6}$$

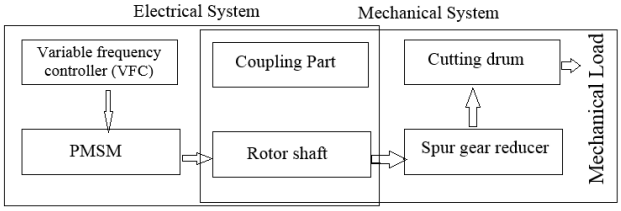

Fig. 1: Semi-direct Shearer Drive Cutting Transmission Mechanism

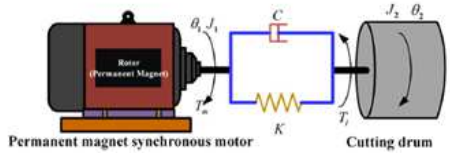

Fig. 2: Physical model of electromechanical coupling transmission system of shearer

Solution of equation (5) is:

$$x_0=A(T_1)e^{i\omega T_0}+\bar{A}(T_1)e^{-i\omega T_0}. \tag{7}$$

Substituting from equation (7) into equation (6) and neglecting all secular terms at the instance of sub-harmonic resonance state ($\Omega_2=2\omega+\varepsilon\sigma$) as the worst situation, we have:

$$-2i\omega\dot{A}-i\mu\omega A-3\alpha A^2\bar{A}+\frac{f_2\bar{A}}{2}e^{i\sigma T_1}-k_1 i\omega A=0 \tag{8}$$

Where σ is called the detuning parameter.

Converting A to the polar form, we have:

$$A=\frac{a}{2}e^{i\beta}, \tag{9}$$

where $\beta, and\ a$ are the system phase and amplitude, respectively.

Introducing Equation (9) in Equation (8) and equating the imaginary and the real parts, we get:

$$\dot{a}=\frac{f_2 a\sin(\theta)}{4\omega}-\frac{a}{2}(\mu+k_1), \tag{10}$$

$$a\dot{\theta}=\sigma a-\frac{3\alpha a^3}{4\omega}+\frac{f_2 a\cos(\theta)}{2\omega}, \tag{11}$$

where $\theta=\sigma T_1-2\beta$.

For obtaining the steady state solution, we put $\dot{a}=\dot{\theta}=0$ into Equations (10), (11), then squaring and adding the resultant formulas to have:

$$\frac{9\alpha^2}{16\omega^2}a^4-\frac{3\alpha\sigma}{2\omega}a^2+\sigma^2+\mu^2+k_1^2+2\mu k_1-\frac{f_2^2}{4\omega^2}=0 \tag{12}$$

Equation (12) shows the relation between the system amplitude and phase that can be illustrate numerically in the following section.
Discuss the stability behavior of these solutions as well as, linearizing equations (10), and (11) according to Lyapunov first (indirect) method to have the following system:

$$\begin{bmatrix} \dot{a} \\ \dot{\theta} \end{bmatrix} = J \begin{bmatrix} a \\ \theta \end{bmatrix}, \tag{13}$$

$$J = \begin{bmatrix} J_{11} & J_{12} \\ J_{21} & J_{22} \end{bmatrix} = \begin{bmatrix} \frac{\partial \dot{a}}{\partial a} & \frac{\partial \dot{a}}{\partial \theta} \\ \frac{\partial \dot{\theta}}{\partial a} & \frac{\partial \dot{\theta}}{\partial \theta} \end{bmatrix} \tag{14}$$

where

$$\begin{aligned} J_{11} &= \frac{\partial \dot{a}}{\partial a} = \frac{-1}{2}(\mu + k_1) + \frac{f_2 \sin(\theta)}{4\omega}, \\ J_{12} &= \frac{\partial \dot{a}}{\partial \theta} = \frac{f_2 a \cos(\theta)}{4\omega}, \\ J_{21} &= \frac{\partial \dot{\theta}}{\partial a} = \frac{\sigma}{a} - \frac{9\alpha a}{4\omega} + \frac{f_2 \cos(\theta)}{2\omega a}, \\ J_{22} &= \frac{\partial \dot{\theta}}{\partial \theta} = -\frac{f_2 \sin(\theta)}{2\omega}. \end{aligned} \tag{15}$$

Thus consistency of the steady-state solution varies based on the analysis of the Jacobian matrix characteristic equation that can be obtained by:

$$\begin{vmatrix} J_{11} - \lambda & J_{12} \\ J_{21} & J_{22} - \lambda \end{vmatrix} = 0, \tag{16}$$

or

$$\lambda^2 + H_1 \lambda + H_2 = 0, \tag{17}$$

where

$$\begin{aligned} H_1 &= -(J_{11} + J_{22}), \\ H_2 &= J_{11} J_{22} - J_{12} J_{21}. \end{aligned} \tag{18}$$

The state's solution is asymptotically stable, as seen by the Routh-Huriwitz criterion, if and only if all real parts for roots of Eq. (17) are both negative This condition is occurred if the coefficients satisfy $H_1 > 0$, *and* $H_2 > 0$,. These conditions are discussed numerically.

3 Numerical simulations and discussion

Simulation results are summarized in this part to verify the analytical calculation earlier. The fourth order Rung-Kutta method (RKM) has been used to estimate the numerical result of the module given, assuming the following parameters:

$$\mu = 0.3,\ \alpha = 0.4,\ \gamma = 0.2,\ f_1 = 2.5,\ f_2 = 7.$$

Figure 3 (a, b) shows the time response and system phase plane respectively with non-resonant case at $\omega = 5$, $\Omega_1 = 13$, $\Omega_2 = 8$, and without control ($k_1 = 0$). Figure 4 demonstrates the time response for the scheme in the instance of implementing the primary resonance $\Omega_1 = 2\omega_1 + \varepsilon\sigma_1$, without applying any control scheme and $\omega = 5$. We observe that the amplitude is increases to the value 1.537. however, in Figure 5, the amplitude is

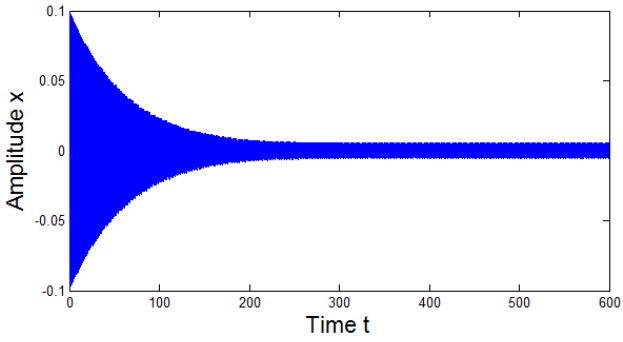

The time response solution at $k_1 = 0$, and at basic case.

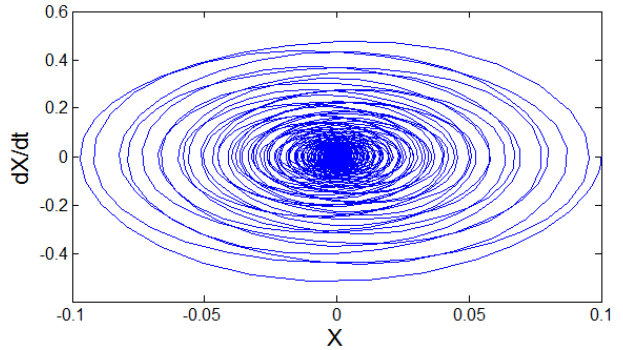

System phase plane, at $k_1 = 0$, and at basic case.

Fig. 3: Response solution at non-resonance case and without applying control

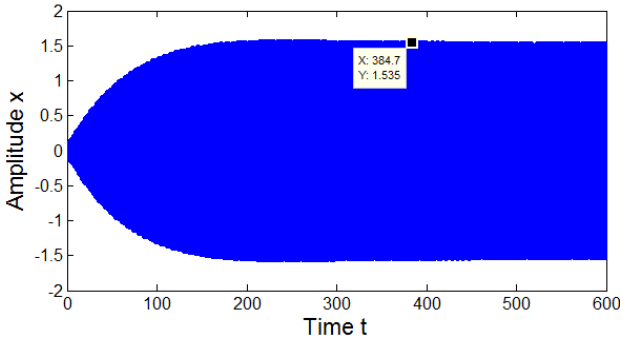

Fig. 4: The time response solution with primary resonance case $\Omega_1 = \omega + \varepsilon\sigma_1$, $\omega = 5$, $\Omega_2 = 8$, $k_1 = 0$.

increases to the value 3.228 in case of applying sub-harmonic resonance case $\Omega_2 = 2\omega + \varepsilon\sigma$, without control, $\omega = 5$, and $\Omega_1 = 13$,. Hence the worst resonance case is the sub-harmonic resonance case

($\omega : \Omega_2 \approx 1 : 2$). We applied cubic velocity feed-back (CVFBC) and velocity feed-back control (VFBC) for this worst resonance case in figures 6 and 7, respectively. We found that the amplitude reduced by 96.7 % due to the effect of the cubic velocity feed-back control (CVFBC) represented by $(-k_1 \dot{x}^3)$. Whereas it reduced by 99.95%

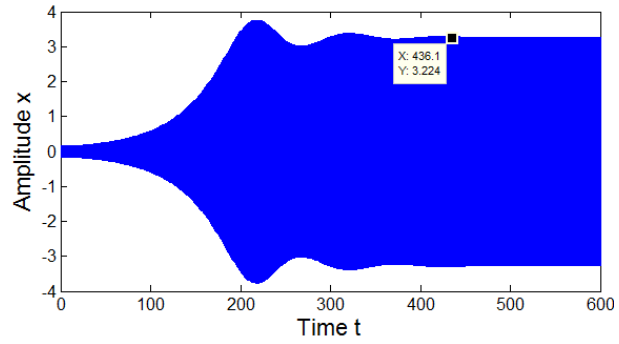

Fig. 5: The time response solution with sub-harmonic resonance case
$\Omega_2 = 2\omega + \varepsilon\sigma$, $\omega = 5$, $\Omega_1 = 13$, $k_1 = 0$.

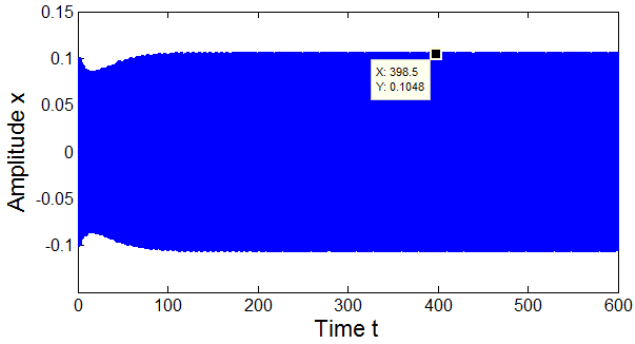

Fig. 6: The time response solution with applying cubic velocity feed-back control (CVFBC) at sub-harmonic resonance case $\Omega_2 = 2\omega + \varepsilon\sigma$, $\omega = 5$, $\Omega_1 = 13$, $k_1 = 0.5$.Controller effect is about 96.7%.

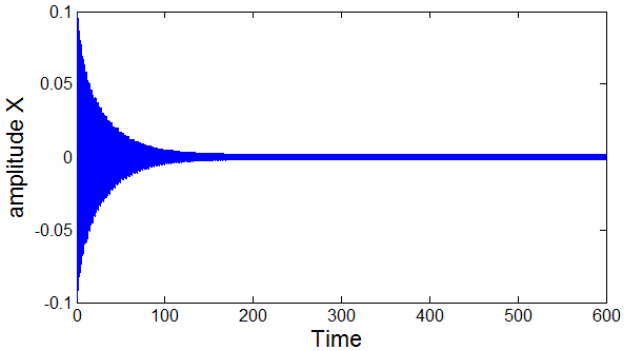

Fig. 7: The time response solution with applying velocity feed-back control (VFBC) at sub-harmonic resonance case $\Omega_2 = 2\omega + \varepsilon\sigma$, $\omega = 5$, $\Omega_1 = 13$, $k_1 = 0.5$.Controller effect is about 99.95%.

after applying velocity feed-back control (VFBC)

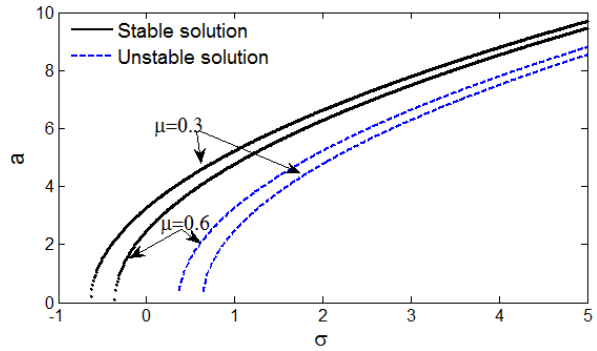

Fig. 8: Frequency response curves at μ =0.3, and 0.6 at sub-harmonic resonance case $\Omega_2 = 2\omega + \varepsilon\sigma$, $\omega = 5$, $\Omega_1 = 13$, $k_1 = 0$. Stable solution: black curve, Unstable solution: blue curve.

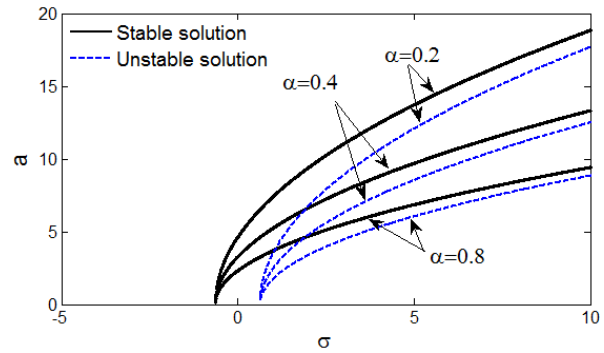

Fig. 9: Frequency response curves at $\alpha = 0.2, 0.4, 0.6$, and 0.8 at sub-harmonic resonance case $\Omega_2 = 2\omega + \varepsilon\sigma$, $\omega = 5$, $\Omega_1 = 13$, $k_1 = 0$. Stable solution: black curve, Unstable solution: blue curve.

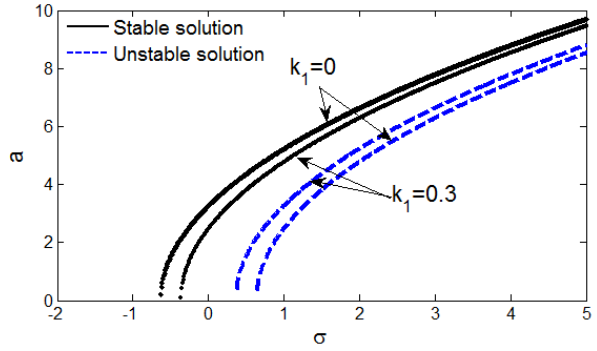

Fig. 10: Frequency response curves at $k_1 = 0$, and 0.3 at sub-harmonic resonance case $\Omega_2 = 2\omega + \varepsilon\sigma$, $\omega = 5$, $\Omega_1 = 13$. Stable solution: black curve, Unstable solution: blue curve.

represented by $(-k_1\dot{x})$. Obviously, (VFBC) is more effective than the (CVFBC), so we supported the adoption of (VFBC) in this system. The scheme parameters impact

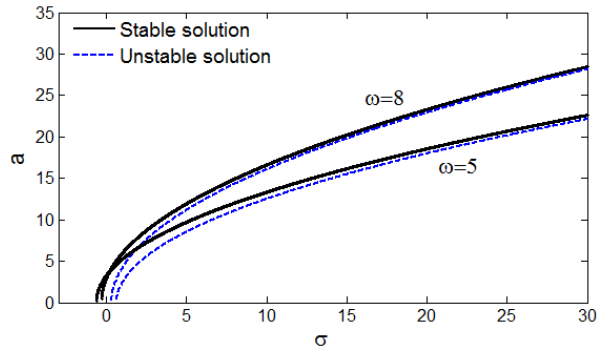

Fig. 11: Frequency response curves at $\omega = 5$, and 8at sub-harmonic resonance case $\Omega_2 = 2\omega + \varepsilon\sigma$, $\Omega_1 = 13$, and $k_1 = 0$. Stable solution: black curve, Unstable solution: blue curve.

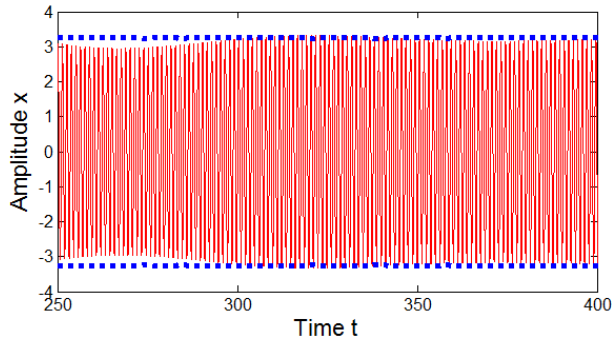

Fig. 12: Comparison between analytic results (red curve) and approximate solution (blue curve) for the time response at sub-harmonic resonance case $\Omega_2 = 2\omega + \varepsilon\sigma$, $\omega = 5$, $\Omega_1 = 13$, and $k_1 = 0$.

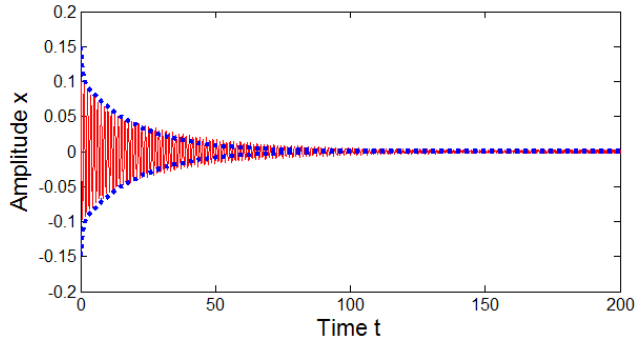

Fig. 13: Comparison between analytic results (red curve) and approximate solution (blue curve) for the time response at sub-harmonic resonance case and VFBC, $\Omega_2 = 2\omega + \varepsilon\sigma$, $\omega = 5$, $\Omega_1 = 13$, and $k_1 = 0.5$.

on the response curves are clarified by figures 8 and 9 at sub-harmonic resonance. In figure 8, the parameter

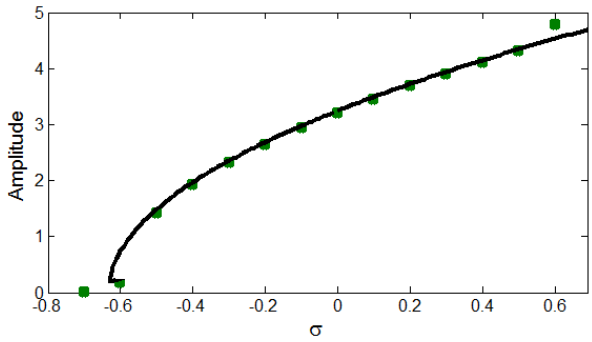

Fig. 14: Comparison between approximate results (black curve) and RKM solution (green curve) for the frequency response at sub-harmonic resonance case, $\Omega_2 = 2\omega + \varepsilon\sigma$, $\omega = 5$, $\Omega_1 = 13$, and $k_1 = 0$.

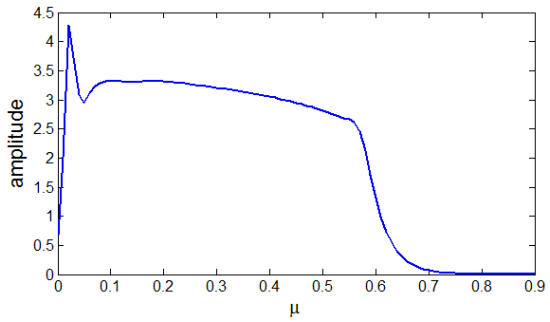

Fig. 15: Effect of damping coefficient μ on system amplitude at sub-harmonic resonance case, $\Omega_2 = 2\omega + \varepsilon\sigma$, $\omega = 5$, $\Omega_1 = 13$, and $k_1 = 0$.

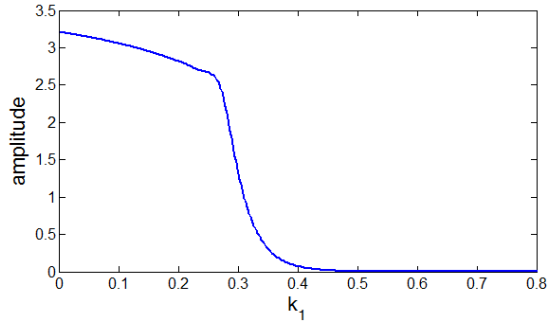

Fig. 16: Effect of VFBC gain $k_1$on system amplitude at sub-harmonic resonance case, $\Omega_2 = 2\omega + \varepsilon\sigma$, $\omega = 5$, and $\Omega_1 = 13$.

$\mu = 0.3, 0.6$ is used, where $\alpha = 0.2, 0.4, 0.6$ and 0.8 is used in the MATLAB program for figure 9. The effect of controller gain and the internal frequency on the amplitude is shown in figures 10 and 11 respectively. We observe in these figures that system amplitude is proportional inversely with varying the damping parameterμ , the cubic term coefficientα, controller

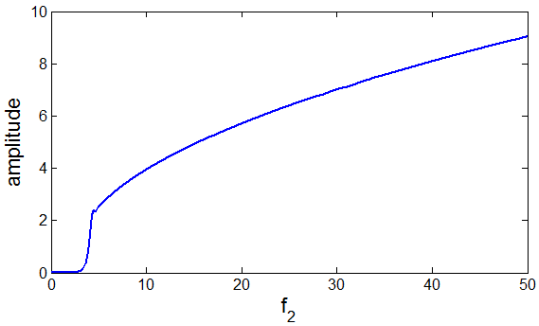

Fig. 17: Effect of VFBC gain $f_2$on system amplitude at sub-harmonic resonance case, $\Omega_2 = 2\omega + \varepsilon\sigma$, $\omega = 5$, and $\Omega_1 = 13$.

Table 1: Comparative analysis of the outcomes of the numerical solution using RKM and the estimated solution for the model without control using MTSM for Fig. 14.

Sigma (σ)	RKM	MTSM	Absolute Error
-0.55	1.0448	1.1723	0.1275
-0.5	1.421	1.4858	0.0648
-0.45	1.6944	1.7438	0.0494
-0.4	1.9174	1.9683	0.0509
-0.35	2.1243	2.1697	0.0454
-0.3	2.3176	2.3539	0.0363
-0.25	2.4805	2.5247	0.0442
-0.2	2.6432	2.6847	0.0415
-0.15	2.7967	2.8357	0.039
-0.1	2.9401	2.979	0.0389
-0.05	3.0749	3.1157	0.0408
0	3.206	3.2467	0.0407
0.05	3.334	3.3726	0.0386
0.1	3.457	3.4939	0.0369
0.15	3.5751	3.6112	0.0361
0.2	3.6891	3.7248	0.0357
0.25	3.7988	3.835	0.0362
0.3	3.9063	3.9422	0.0359
0.35	4.0111	4.0465	0.0354
0.4	4.1157	4.1482	0.0325
0.45	4.2177	4.2475	0.0298
0.5	4.3057	4.3445	0.0388
0.55	4.4399	4.4393	0.0006

gaink_1, and the internal frequencyω. Stable and unstable regions are represented by the black and blue curves respectively. Both solution induced by (MTSM) and numerical solution using Rung-Kutta Method (RKM) of fourth order are compared in figures 12-14 for time history and frequency response curves for the system. These figures show good agreement between the approximate solution (blue curve) and the numerical result (red curve) of equation of the system in case of $k_1 = 0$(figure 12) and $k_1 = 0.5$for (VFBC) (figure 13) at sub-harmonic resonance case. Figure 14 provides good results between the used methods (MTSM and RKM) for the frequency response. We observed that the study shows that all numerical solution projections are in good alignment with computational solutions (see Tables 1). The change of amplitude range with varying of the system parameters is illustrated in figures 15-17. We observe that the amplitude is reverse related with the value of μ ,and the control gain k_1 as shown in figures (15) and (16), respectively. In contrast, it is direct proportional with the force f_2 up to reaching saturation case as shown in figure (17).

4 Conclusion

In this study, using multiple time scales methodology, a dynamical dynamic model of the shearer permanent magnetic moderately drive breaking transmission mechanism with multi-excitation forces was reviewed and solved. Also, the disastrous resonance incidents through VFBC and CVFBC were addressed. The worse situation of resonance is sub-harmonic case under these excitations i.e.$\Omega_2 : \omega = 2 : 1$. The influence of VFBC and CVFBC was clarified. It was shown that control effect is about 99.95% due to the outcome of VFBC, and about 96.7 % due to the effect of the CVFBC. Consequently, the VFBC is more effective for this system under the effect of external and parametric excitation forces. In order to minimize the amplitude peak and improve the stability area, an appropriate stability analysis was also conducted and appropriate choices were found for the feedback gains. Moreover, approximate solutions obtained by the multiple-scale method) were compared with numerical solutions using the fourth-order Rung-Kutta method. The distinction offered a good agreement between approximate and numerical approaches. Finally, the effect of electromagnetic factors on the scheme amplitude and its consequence on stability criteria for the system were premeditated.

Acknowledgement

The authors would like to thank the anonymous referee for the constructive comments that improved the paper.

Conflict of Interest

The authors declare that there is no conflict of interest regarding the publication of this paper.

References

[1] J. Xu, Z. Wang, C. Tan, L. Si, and X. Liu. Cutting pattern identification for coal mining shearer through a swarm intelligence-based variable translation wavelet neural network. *Sensors 18(2)*, 382, 2018.

[2] W. Wei, H. Liang, T. Wuest, and A. Liu. *A new module partition method based on the criterion and noise functions of robust design*. Int. J. Adv. Manuf. Technol, 2016.
[3] N. Bilgin, M. A. Demircin, H. Copur, C. Balci, H. Tuncdemir, and N. Akcin. Dominant rock properties affecting the performance of conical picks and the comparison of some experimental and theoretical results. *Int. J. RockMech. Min*, 43(1), 2006.
[4] C. Zhu, X. Lu, Z. Gao, F. Yan, C. Guo, and X. Zhang. Effect of high-voltage thermal breakdown on pore characteristics of coal. *Int. J. Min. Sci. Technol*, 27(6), 2017.
[5] L. Sheng, W. Li, Y. Wang, M. Fan, and X. *Yang: Sensorless control of a shearer short-range cutting interior permanent magnet synchronous motor based on a new sliding mode observer*. 2017.
[6] W. Tao, C. Chen, J. Han, and T. Ren. Effect of bolt rib spacing on load transfer mechanism. *Int. J. Min. Sci. Technol*, 27(3), 2017.
[7] K. Liu and Z. Q. Zhu. Online estimation of the rotor flux linkage and voltage-source inverter nonlinearity in permanent magnet synchronous machine drives. *IEEE Trans. Power Electron*, 29(1), 2013.
[8] Q. Wei and X. Y. Wang. Chaos controlling of permanent magnet synchronous motor base on dither signal. *J. Vib. Control*, 19(16), 2013.
[9] X. Chen, S. Yuan, and Z. Peng. *Nonlinear vibration for pmsm used in hev considering mechanical and magnetic coupling effects*. Nonlinear Dyn, 2015.
[10] R. Shan mug asundram. *K. M. Zakariah, and N. Yadaiah, Effect of parameter variations on the performance of direct current (dc) servomotor drives. J. Vib. Control*, 19(19), 2013.
[11] H. J. Shin, J. Y. Choi, H. I. Park, and S. M. Jang. Vibration analysis and measurements through prediction of electromagnetic vibration sources of permanent magnet synchronous motor based on analytical magnetic field calculations. *IEEE Trans. Magn*, 48(11), 2012.
[12] J. Ju, W. Li, Y. Wang, M. Fan, and X. Yang. Dynamics and nonlinear feedback control for torsional vibration bifurcation in main transmission system of scraper conveyor directdriven by high-power pmsm. *Nonlinear Dyn*, 93(2), 2018.
[13] Y. A. Amer, A. T. El-Sayed, and F. T. El-Bahrawy. Torsional vibration reduction for rolling mill's main drive system via negative velocity feedback under parametric excitation. *J. Mech. Sci. Technol*, 29(4), 2015.
[14] Y. Yi, D. Qin, and C. Liu. Investigation of electromechanical coupling vibration characteristics of an electric drive multistage gear system. *Mech. Mach. Theory*, 121, 2018.
[15] X. Yang, H. Liu, D. Lu, and W. Zhao. Investigation of the dynamic electromechanical coupling due to the thrust harmonics in the linear motor feed system. *Mech. Syst. Signal Process*, 111, 2018.
[16] L. Xu and Y. Gao. Bifurcation and chaotic vibration in electromechanical integrated toroidal drive. *J. Vib. Control*, 21(8), 2013.
[17] W. Bai, D. Qin, Y. Wang, and T. C. Lim. Dynamic characteristic of electromechanical coupling effects in motor-gear system. *J. Sound Vib.*, 423, 50–64, 2018.
[18] T. Szolc, R. Konowrocki, M. Michajłow, and A. Pregowska. An investigation of the dynamic electromechanical coupling effects in machine drive systems driven by asynchronous motors. *Mech. Syst. Signal Process*, 49(2), 2014.
[19] Y. Calleecharan and J. O. Aidanpaa. Stability analysis of an hydropower generator subjected to unbalanced magnetic pull. *IET Sci. Meas. Technol*, 5(6), 2011.
[20] R. K. Gustavsson and J. O. Aidanpää. The influence of nonlinear magnetic pull on hydropower generator rotors. *J. Sound Vib*, 297(3), 2006.
[21] N. L. P. Lundström and J. O. Aidanpää. *Dynamic consequences of electromagnetic pull due to deviations in generator shape*. J, 2007.
[22] Z. Song and Z. Ma. Nonlinear vibration analysis of an eccentric rotor with unbalance magnetic pull. *J. Vib. Shock*, 29(8), 2010.
[23] Z. Huang, J. Zhou, M. Yang, and Y. Zhang. Vibration characteristics of a hydraulic generator unit rotor system with parallel misalignment and rub-impact. *Arch. Appl. Mech*, 81(7), 2011.
[24] L. Ran, D. Xiang, and J. L. Kirtley. Analysis of electromechanical interactions in a flywheel system with a doubly fed induction machine. *IEEE Trans. Ind. Appl*, 47(3), 2011.
[25] J. Zhong and H. Tang. Vibration problems of high speed rolling mill-study of dynamics of complex electromechanically coupled system. *J.Vib. Meas. Diagn*, 22(1), 2002.
[26] C. B. Gan, Y. H. Wang, S. X. Yang, and Y. L. Cao. Nonparametric modeling and vibration analysis of uncertain jeffcott rotor with disc offset. *Int. J. Mech. Sci*, 78(1), 2014.
[27] K. Chen, J. Hu, and Z. Peng. Analysis of torsional vibration in an electromechanical transmission system. *Adv. Mech. Eng.*, 8(6), 2016.
[28] Y. S. Hamed, A. El Shehry, and M. Sayed. Nonlinear modified positive position feedback control of cantilever beam system carrying an intermediate lumped mass. 59(5), 2020.
[29] Lianchao Sheng, Wei Li, Song Jiang, Jiajun Chen, and Ang Liu. *Nonlinear torsional vibration analysis of motor rotor system in shearer semi-direct drive cutting unit under electromagnetic and load excitation*. Nonlinear Dyn., 2019.

Yasser A. Amer received his B.S. degree in Mathematics from Zagazig University, EGYPT, in 1992. He then received his M.S.c and Ph.D. degrees from Zagazig University, in 1996 and 2002, respectively. Dr. Y. A. Amer is currently an full Professor of Mathematics at the Department of Mathematics, Faculty of Science, Zagaziga University, Egypt. Dr. Y. A. Amer research interests include Non-linear dynamical systems, Numerical Analysis, Vibration control and Partial differential equations.

Taher A. Bahnasy is working as a teaching Stuff at Faculty of Engineering, Tanta University Tanta, Egypt. M.Sc. in Differential Equations from Tanta University, Egypt. Thesis title: "Study on Existence and Stability of Solutions of Ordinary and Fractional Differential equations". His research focused on stability of dynamical systems modeled by an ordinary and fractional differential equations. B.Sc. in Electrical Power and Machines, Faculty of Engineering, Tanta University, Egypt, June, 2009 (Excellent with honor). His published research articles in the area of applied mathematics, Non-linear dynamical systems and differential equations.

Ashraf M. Elmhlawy Is a lecturer of engineering mathematics at Tanta University, Egypt. He received his Phd. degree in numerical Solutions of Partial Differential Equations Based on Spline Functions from Tanta University (Egypt). His research interests are in the areas of applied mathematics, numerical simulations, and pure mathematics. He published research articles in the area of applied mathematics and numerical solutions for some mathematical models.